

19. Meter, D. M., Ph.D. thesis, Univ. of Wisconsin, Madison, Wisconsin (1963).
20. ———, *A.I.Ch.E. Journal*, **10**, 881-884 (1964).
21. ———, and R. B. Bird, *ibid.*, 878-881.
22. Reiner, M., "Deformation, Strain, and Flow," Interscience, New York (1960).
23. Sadowski, T. J., Ph.D. thesis, Univ. of Wisconsin, Madison, Wisconsin (1963).
24. Slattery, J. C., Ph.D. thesis, Univ. of Wisconsin, Madison, Wisconsin (1959).
25. ———, and R. B. Bird, *Chem. Eng. Sci.*, **16**, 231-241 (1961).
26. Sneddon, I. N., "Elements of Partial Differential Equations," p. 49, McGraw-Hill, New York (1957).
27. Spriggs, T. W., Ph.D. thesis, Univ. of Wisconsin, Madison, Wisconsin (1965).
28. ———, *Chem. Eng. Sci.*, **20** (1965).
29. ———, and R. B. Bird, *Ind. Eng. Chem. Fundamentals*, **4**, 182-186, (1965).
30. Sutterby, J. L., Ph.D. thesis, Univ. of Wisconsin, Madison, Wisconsin (1964).
31. Turian, R. M., Ph.D. thesis, Univ. of Wisconsin, Madison, Wisconsin (1964).
32. Turian, R. M., *Chem. Eng. Sci.*, **20** (1965).
33. Williams, M. C., and R. B. Bird, *Phys. of Fluids*, **5**, 1126 (1962); **6**, 314 (1963).
34. ———, *Ind. Eng. Chem. Fundamentals*, **3**, 42-49 (1964).

Manuscript received August 25, 1964; revision received December 21, 1964; paper accepted December 23, 1964.

Flash X-Ray Analysis of Fluidized Beds

JACOB B. ROMERO and DON W. SMITH

The Boeing Company, Seattle, Washington

Flash X-ray radiography was used to study the internal structure of fluidized beds. Basic data were obtained on the density distribution and on void shapes, sizes, and velocities within an air-sand bed. The data obtained, in general, support the view of fluidized beds as consisting of liquidlike emulsions through which voids rise. Density measurements and void characteristics were in agreement with the two-phase flow theory and with more recent theories of fluid bed flow. Void velocities and shapes agreed with recent predictions that the dense phase behaves as a liquidlike emulsion of zero viscosity and surface tension.

A fruitful model of a gas fluidized bed depicts it as consisting of a stable, liquidlike dense phase through which voids rise. The void maintains its integrity through gas circulation that enters through its base and exits through its roof and sides. Essentially, all fluid not required to fluidize the bed bypasses the bed in the form of voids. This concept has contributed greatly to a basic understanding of the fluidized bed. It is now possible to predict many properties of the fluid bed—mode of fluidization (1), bed stability (2), void movement (3, 4), and solid mixing (5)—with a fair degree of success.

The model of the fluidized bed described above combines the simplicity of the two-phase flow theory (6) with theories to account for void stability and flow. The main purpose of the present study was to obtain experimental data in support of these theories through a study of dense- and dilute-phase characteristics. For example, a knowledge of density distribution should provide evidence for the validity of the two-phase flow theory. Also, measurements of bubble shapes, sizes, and velocities should help support theories on flow of voids through fluidized solids.

Previous experiments on fluidized beds have, in general, supported this model, but have also counted heavily on observations near the wall surfaces of fluidized beds and on probe measurements inserted into the bed. The latter measurements have used capacitance probes (7), light probes (8), and localized X-ray beams (9). Dye has been used to produce streak lines around voids in two-dimensional beds and thereby illustrate the flow pattern (10). Bubble velocities have been measured by introducing gas pulses, which are not indigenous to the bed, into a bed held just above minimum fluidization (11, 12).

In the present study, flash X-ray radiography was used to study the internal structure of fluidized beds (13). In this manner, the motion within the bed was stopped, and it was possible to observe conditions existing within a large section of the bed without disturbing the bed in any manner. Flash X-ray photographs yielded data on density distribution, bubble sizes, and bubble shapes. Two flash units fired in sequence permitted measurement of the velocity of bubbles as they rise through the bed. The flash X-ray machine has an extremely fast exposure time; this feature can be used to advantage in experiments where fast motion has to be resolved. Previous applications of flash X-ray include the resolution of motion of bullets, expansion of exploding wires, and displacement of internal organs during acceleration (14).

The work was essentially statistical. To obtain data on bubble sizes, for instance, many measurements were undertaken to obtain a statistical average. Because of these and other considerations, this work was limited to an air-sand system and to one column size. The results, which support many previous theories, should prove valuable for a basic understanding of fluidized beds and should provide useful data for fluid bed design.

EXPERIMENTAL

Apparatus

Two existing flash X-ray facilities were used to obtain photographs of the bed internals. These units, which are designed for 300- and 600-kv. operation, could easily penetrate a few inches of solid fluidized material. Except for experiments involving void velocity measurements, only the 300-kv. unit was used.

The basic elements of the flash X-ray unit are a specially designed tube and an energy storage bank. Additional equipment consists of spark gap switches for firing the unit, and charging, control, and radiation monitoring equipment. The heart of a flash X-ray unit is the flash tube, which operates on the field-emission principle, firing a square pulse of about 0.2 μ sec. duration. In the present setup, these tubes are mounted on opposite walls of an 8 x 12 x 8 ft. lead-lined room, firing into the room through portholes. The energy storage banks consist of delay lines that are charged in parallel and discharged in series, thus making a high-voltage pulse possible. The storage banks for the 300-kv. unit, for example, consist of six banks, each made of a 66 ft. long copper wire. These are charged to 100 kv. each giving 600 kv. upon series discharge; impedance in the system reduces this to 300 kv. at the tube. The current pulse is about 1,000 amp.

A 3-in. sq. Plexiglas column contained the fluidized material. Details of this device are given in Figure 1. The main column, which was 20 $\frac{1}{4}$ in. high, was attached to a 6 $\frac{3}{8}$ in. calming section filled with 5-mm. glass beads. The two sides of the column parallel to the X-ray beam direction were $\frac{3}{8}$ in. thick and served as a density reference; the sides perpendicular to the beam were only 1/16 in. thick so as to avoid excessive X-ray absorption. The sand rested on a 300-mesh bronze screen distributor, which was further supported by a heavier screen. Laboratory air flow rate was controlled by a pressure-reducing valve and a gate valve and was then metered through rotameters before entering the column.

Experimentation with several types of films revealed that royal blue medical film gave the best contrast. The 8 x 10 in. sheets of film were mounted inside light intensifier cassettes. A means of comparing film darkness had to be devised to obtain quantitative density data. A special photo densitometer accomplished this comparison. It consisted of a photo pickup cell, light source, and carriage for mounting the film. The light pickup was a photocell with an active area of 0.25 x 0.5 in. The light source was produced by a voltage-regulated projection lamp. This illuminated the film from below, and the transmitted beam was passed through a $\frac{1}{8}$ x 0.001 in. slit before reaching the photocell.

The film was mounted between glass surfaces in a carriage (from an old commercial photo densitometer) that moves laterally and longitudinally. The photocell output operated the X axis of an autograph X-Y recorder; the carriage position, through a resistor arrangement, operated the Y axis. In this manner, film darkness and position were recorded automatically.

To measure void velocity, the two X-ray units were fired in sequence a few tenths of a second apart. The experimental arrangement used for these measurements is shown in Figure 2. Two cassettes with film were mounted on opposite sides of the column; one X-rayed the upper portion of the bed and the other the lower portion. Each cassette was backed by a 1 in. thick lead shield, thereby masking out the effects of the X-ray unit fired from its side. With reference to Figure 2, the 300-kv. unit was fired first, and the bottom part of the bed was photographed. A few tenths of a second later, the 600-kv. unit was fired, and the upper part of the bed was photographed. Voids that traveled from the bottom to the top showed in both photographs, and the distance traveled was measured. The

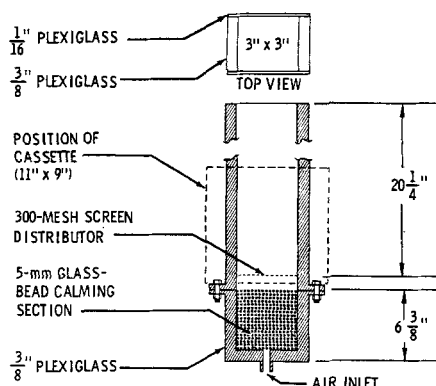


Fig. 1. Fluidization column details.

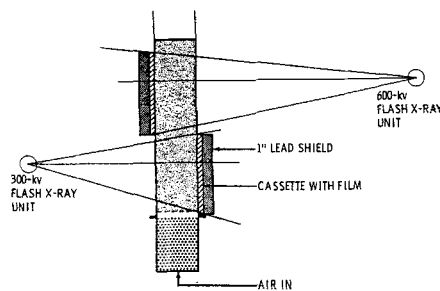


Fig. 2. Scheme for measuring void velocity.

exact time between firings was measured by a 1-megacycle timer; when the distance a void had traveled and the time interval were known, its velocity was determined directly.

The main sources of error in film density measurements were variations in X-ray operating voltage, variations in spatial uniformity of the X-ray beam intensity, variations introduced during film development, and variations in the film itself. Although care was taken to minimize these sources of error, it was found that the variation was great enough to preclude fine comparisons of density between photographs. To eliminate these errors, a scheme was devised by which each photograph could be individually compared with a standard. The standards were sandfilled wedges constructed of 1/16 in. thick Plexiglas walls. They were right triangular, 3 x 4 x 5 in., and were filled with sand to a density of 88 lb./cu. ft. These were mounted on the side of the fluidizing column so that an X-ray photograph of them was obtained when the X-ray was fired. The wedge gave a film darkness gradation which could be related to actual sand thickness. By comparing film darkness in the wedge with darkness in the bed, local density could be obtained throughout the bed.

Materials

Air at room temperature and normal atmospheric pressure was used for fluidization. All data were obtained on a white silica sand which was approximately spherical. The sand density, 146 lb./cu. ft., was determined by water displacement. The minimum fluidization velocity, 0.056 ft./sec., was determined by measuring pressure drop vs. flow rate. A size analysis of the sand indicated that it had a large fraction passing the 150-Tyler-mesh screen; some 70% of the sand by weight was retained by the mesh range 150 to 200. The true arithmetic average diameter was 0.0028 in. Results of the screen analysis are tabulated below.

Tyler mesh	Weight fraction	Average particle diameter (in.)
+ 60	0.011	0.0097
- 60 + 100	0.027	0.0078
-100 + 150	0.010	0.0050
-150 + 200	0.692	0.0035
-200 + 270	0.143	0.0025
-270	0.117	0.0021

Procedure

To make a run, the fluidizing apparatus was placed inside the flash X-ray radiation room. In experiments that required only the 300 kv. X-ray machine, the fluidizing column was placed directly in front of the tube porthole, 5 ft. 8 in. from its front face, and elevated to about the level of the tube. This placed the column in a fairly uniform section of the beam. In experiments that required both machines (void velocity measurements), the column was placed in a line joining the two X-ray tubes about 2 ft. from the front face of the 300-kv. tube. A known weight of sand was placed in the tube, and air was metered through the bed at the desired flow rate. The cassette containing the film was then mounted in position, and the flash X-ray machine was charged and fired. Bed heights of 3, 6, 11, and 15 in. and flow rates of one, one and a half, two, three, and five times minimum were studied. To obtain statistical data, ten or twelve photographs were taken at each flow

rate (higher than minimum) and at each bed height. In all, some two hundred photographs were taken.

The developed negatives were first examined visually and then scanned for density with the densitometer along vertical lines spaced $\frac{1}{4}$ in. apart. Areas where voids were present were scanned along horizontal lines spaced $\frac{1}{8}$ in. apart. Direct comparison of the $\frac{1}{4}$ in. spaced scanning with the calibration wedge density yielded the bed density. The $\frac{1}{8}$ in. scanning was used in conjunction with void volume calibration to determine void size. To calibrate the densitometer for void volume, photographs were obtained of a ping-pong ball of known size imbedded in a bed operated just below minimum fluidization. A procedure, described in detail in reference 13, was worked out by which the total volume was integrated from the densitometer output. Thus the volume of irregularly shaped voids could be determined. As a check, several dimensions along different axes of the void were measured, and the volume was calculated on the basis of an average. The two methods agreed quite closely.

To measure void velocity, the two photographs were compared for the presence of coincident voids. The distance traveled by voids that appeared in both photographs was measured. From these data and the travel time, the velocity was determined.

RESULTS

Typical flash X-ray photographs of portions of two beds are shown in Figure 3, a sequence taken at two flow rates in beds of $L_{mf} = 11$ in. (This photograph was reproduced from X-ray negatives and, as a result, has lost some detail. Therefore, conclusions drawn by visual inspection might be misleading. In actual practice, the flash X-ray negatives were examined.) Visual inspection of flash X-ray negatives showed that the fluidized bed consisted of two distinct phases, as had previously been postulated. Although quantitative density determination by visual means alone was impossible, inspection of photographs showed quite general dense-phase uniformity (no abrupt density changes) and quite distinct voids. Near the bottom of the bed, however, no distinct voids were present and none were found in the photographs examined. This region seemed to behave as a more or less turbulent area having little definition between phases. This region was probably highly influenced by the distributor and by the flow adjusting to the formation of voids. Further proof of this was supplied by densitometer readings which were in many cases anomalous 0.5 to 1 in. from the distributor. In a few photographs (see Figure 3, for example), the lower

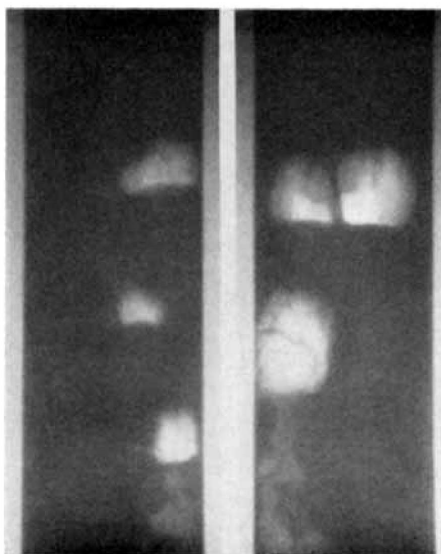


Fig. 3. Flash X-ray photographs of fluidized beds at different flow rates (left hand, $G/G_{mf} = 1.5$; right hand, $G/G_{mf} = 3.0$).

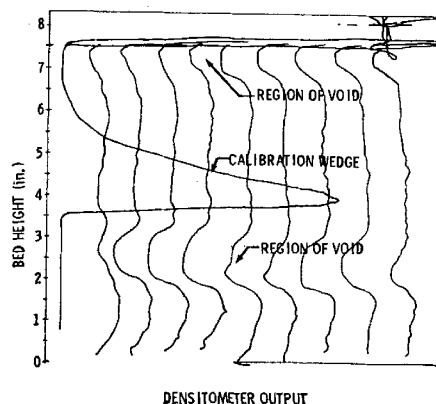


Fig. 4. Densitometer output through typical bed ($G/G_{mf} = 1.5$).

voids indicated what might be streaming into their bottom surface. This phenomenon was probably the result of air being drawn (circulated) through the void.

The void sizes increased with flow rate as had been expected. Even at the minimum fluidization velocity, tiny bubbles some $\frac{1}{8}$ - to $\frac{1}{4}$ -in. diameter were in many cases observed. At low and intermediate flow rates, the bubble cap shape of voids—flat at the bottom and rounded at the top—was observed in many photographs (in agreement with liquidlike theories of fluidized beds). At a flow rate of five times minimum, many voids tended to become irregular; this was probably the result of wall interference, because the void sizes were often comparable to the column dimensions.

Typical density profiles obtained from the photo densitometer measurements of a large section of a bed are shown in Figure 4 for both the bed and the calibration wedge. The bed was scanned along longitudinal lines every $\frac{1}{4}$ in., and the base line of the recorder was moved a constant amount for each scan to avoid lines overlapping each other. As evidenced, the densitometer output is fairly constant in the dense-phase region of the bed and drops considerably where voids are present. In Figure 5, the densitometer output of Figure 4 is interpreted as actual local bed density. It is seen that the dense-phase density does not vary greatly over large regions of the bed. In the region of the voids, however, densities as low as one half those of the dense phase are found. Figure 6 compares a typical densitometer scan taken in the region of a void with that obtained from a ping-pong ball. Note the decrease in density within the void followed by restoration of density to a fairly constant value outside the void proper.

Cases in which both X-ray machines were fired (those used to measure void velocity) often yielded other useful results besides void velocity. In a few cases voids in the process of combination were observed in the bottom photograph. The combination apparently succeeded, because the upper photograph showed only one void. Further proof of this was supplied by the fact that the volume of the upper void was approximately equal to the volume of the two voids in the bottom photographs. In general, photographs of this nature revealed that voids retained a fairly constant volume throughout their travel; once formed, the void tended to maintain constant size. Other useful information obtained was the path followed by voids. Generally, voids followed straight paths, although in a few cases lateral displacements were observed.

Two-Phase Flow Theory Test

The two-phase flow theory, first proposed in 1952 by Toomey and Johnstone (6), states that all excess fluid,

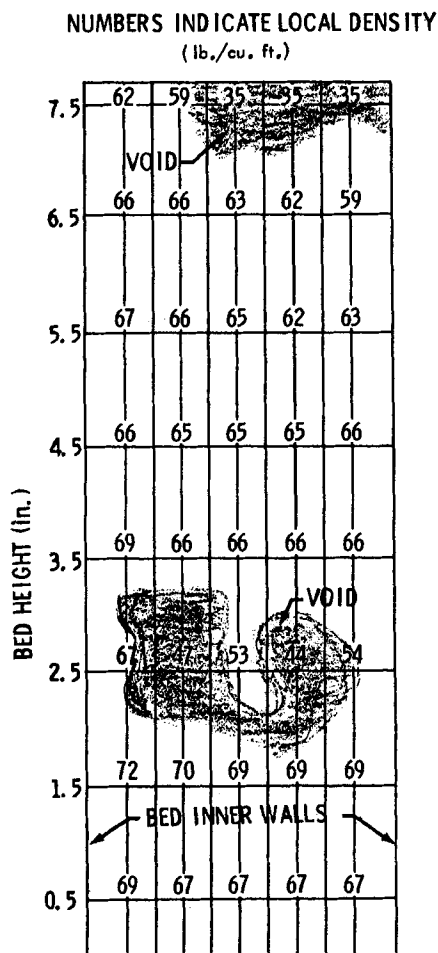


Fig. 5. Map of local density through region of a fluidized bed.

above minimum fluidization, bypasses the bed as voids. Interpreted another way, the theory states that the dense phase should maintain constant density, equal to the density at minimum fluidization, independent of flow rate. As the flow rate is increased, the voids should become larger (and perhaps the frequency should also increase) to accommodate the excess flow. This theory can still be consistent with newer theories of void stability, which propose that the voids maintain their integrity through circulatory flow. In this view, the excess flow bypasses the bed in the sense that a dilute phase exists as voids throughout; however, the fluid in the voids circulates through the dense phase as the void rises.

From the present research, three pieces of evidence support the two-phase flow theory: the void sizes increase with increased flow rate; the void volume, except where combinations occur, tends to remain constant with height; and the dense phase, on the average, maintains a constant density with flow rate equal to that at minimum fluidization.

Increased void size is only of qualitative significance because no independent void frequency measurements were taken. However, the tendency of voids to increase in size is consistent with the two-phase theory. Constant void volume indicates that the flow through the dilute and dense phases is constant throughout the bed. That is, there is no tendency for the two-phase flow theory to be valid at one height of the bed and not valid at another. Although circulation between phases might exist, the average flow rates through the two phases remain constant.

Finally, the most important piece of evidence to support the two-phase flow theory was supplied through density

measurements of the dense phase as a function of flow rate. This evidence is in quantitative agreement with the theory. In the present work, variations of density were measured to a flow rate five times minimum fluidization. These were compared with the density at minimum fluidization. The densities of the individual photographs varied from 62 to 70 lb./cu. ft. When these were averaged for each flow rate, the results shown in Figure 7 were obtained. As can be seen, the dense phase on the average maintains a constant density (with variation of flow rate) equal to the density at minimum fluidization. These data agree quite well with those calculated by bed-height measurements at minimum fluidization. For comparison, the expected density variation when 10% and when 100% of the excess gas is passed through the dense phase was calculated. This calculation was based on the theory of Ergun and Orning (15), assuming that the bed expands in particulate fashion in accordance with the flow through the dense phase. The results obtained here are seen to be consistent with the theory that at least a large portion of the excess gas bypasses; this directly supports the two-phase flow theory.

The variations between individual photographs, which varied from 62 to 70 lb./cu. ft., are consistent with the accuracy of the measurements (which was within about 5%) and also with the fact that slight density transients might exist in the fluidized bed owing to large voids bursting at its surface. This latter effect can be visually observed in slugging beds. As the slug bursts at the surface, a slight compression of the bed followed by an expansion occurs. Slight compressions of this type can also be expected when voids burst at the surface. The X-ray firing can take place at any time during the transient phase, and the photograph might show slightly higher or lower density than the average. However, on the average, the density of the bed should, and did, correspond to that predicted by the two-phase theory.

Void Characteristics

The characteristics of voids were in general agreement with previous experiments and postulates (2, 3, 6, 8, 10, 11, 12). In general, the void size increased with increased flow rate, although above a rate three times minimum, the average size appeared to level off. Bed height had little effect on void size. Although coalescence of voids was observed in some photographs, it occurred infrequently and apparently was not significant in determining void size over the bed heights studied. On the assumption that the two-phase theory holds, void frequencies have been calculated from the relationship $f = 6(w - w_{mf})/\pi y^2 \rho$. The range of frequencies is in quantitative agreement with previous measurements (8); it increases with in-

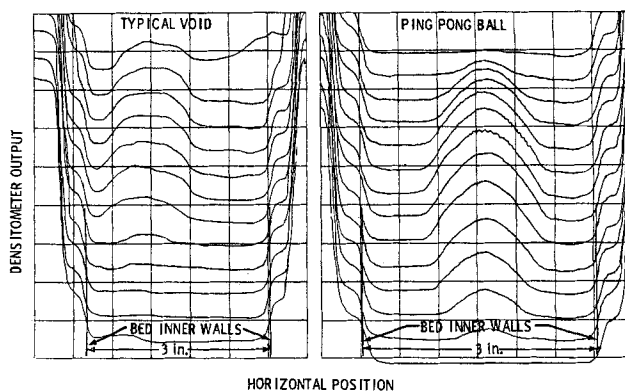


Fig. 6. Densitometer output in the region of a void and a ping-pong ball.

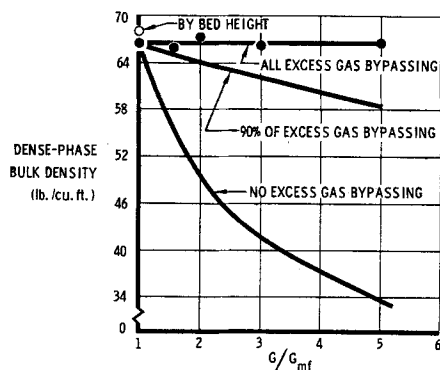


Fig. 7. Dense-phase average density.

creases in flow rate. The table below tabulates average void sizes and frequencies for the various cases studied.

G/G_{mf}	L_{mf} (in.)	(Two-phase flow)	
		Average bubble volume (cu. in.)	Bubble frequency (No./sec./sq. ft.)
1.5	3.1	0.68	72
1.5	5.9	0.50	97
1.5	10.8	0.51	97
3.0	3.1	2.3	85
3.0	5.9	1.3	149
3.0	10.8	1.7	114
5.0	3.1	1.3	300
5.0	5.9	1.9	200

Existing void size data (8) were correlated previously (16) with a standard deviation of 13% by the simple equation $y/z = 0.316(v - v_{mf})^{0.536}$. The data obtained in this study (black dots) are plotted and compared with this equation in Figure 8; these data are some five or more orders of magnitude larger.

The discrepancy between probe and photographic measurements is probably to be expected, because the probe method does not measure maximum vertical dimension or horizontal dimension. A further complication is the different distributors used in each experiment. This latter problem, which necessitates further study, could adversely affect void sizes.

The void shapes observed varied from highly irregular to fairly regular. At the intermediate and low flow rates, the bubble-cap shape (flat bottom and rounded top) was observed in many cases. This seems to be consistent with the inviscid, zero surface tension liquid concept of fluidized beds. At high flow rates, the void shapes were sometimes irregular; however, in this case, the voids had

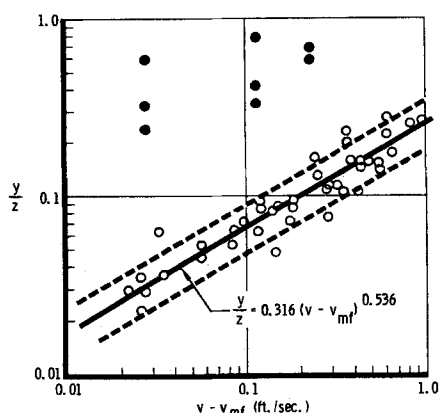


Fig. 8. Void size correlation.

grown to column dimensions so that adverse wall interference was probably present.

Void velocities were also found to be in good agreement with the inviscid, zero surface tension liquid theory of Davies and Taylor (4). This theory predicts that the void velocity should be proportional to the sixth root of the volume. In Figure 9, a plot of velocity vs. $V_B^{1/6}$ is shown, indicating a fairly straight line within experimental error. To a fairly close approximation, these data can be correlated by the relationship $u_B = g^{1/2} V_B^{1/6}$. This might be compared with the relationship suggested by Davies and Taylor: $u_B = 0.792 g^{1/2} V_B^{1/6}$.

DISCUSSION

The results obtained from this study, which support recent theories on fluidization, shed some light on the nature of the fluidized process. As suggested by Rowe (17), the drag on the individual particles is sensitive to particle concentration, and this probably controls to a large extent fluidized bed behavior. Prior to fluidization, the particles are immovable and, as the flow rate is increased, the bed expands simply because this is the path of least resistance. At the minimum fluidization point, the particle weights are balanced by the drag forces, and they become easily movable. In regions where concentration changes occur, one can expect a redistribution of flow because the drag is sensitive even to slight concentration changes (17, 18). One region where this can occur quite frequently is the bottom of the bed, because the distributor is continuously being bombarded by particles, and this undoubtedly results in particle concentration changes. Regions with low concentration receive higher flow, which forms bubbles farther up the bed consistent with the potential theory. Consistent with this view, one would expect a more or less turbulent region near the distributor with no distinct voids yet formed. This effect was observed.

Bed height, unless extreme, has no significant effect on flow. High beds allow more time for void coalescence. Very shallow beds are strongly influenced by the distributor and can behave quite differently from deeper beds. Therefore, it seems dangerous to extrapolate data of very shallow beds to that of deep beds.

The flow of voids in the region of the bed removed from the distributor is consistent with the liquidlike fluidized bed model, and it appears that recent theories on fluidized beds account quite accurately for this phenomenon. Thanks are due mostly to investigators in Great Britain for placing these theories on a firm foundation. In this region of the bed, the dense phase appears to have liquidlike properties, and observations of void shapes and velocities indicate that it approaches a liquid of zero viscosity and surface tensions. Similar previous observations also support this view.

The flow through the bed, at least above the distribution section, is consistent with two-phase flow theory. Apparently, the bed at minimum fluidization is a stable configuration and forms a liquidlike emulsion of constant property. All flow in excess of minimum passing through this emulsion form voids. Perhaps a better view is to think of the excess flow as finding an easier flow path through this liquid by forming voids. As the properties of the fluid are changed (for example, by altering the density and viscosity), the easier path might be the expansion of the bed. This situation has been observed in liquid fluidization of solids.

The results obtained in this study were limited to one system. This system was one with well-established aggregative mode of fluidization, having a ratio of stable void diameter to particle diameter (as defined in reference 1) of around 300. Although there is always danger in ex-

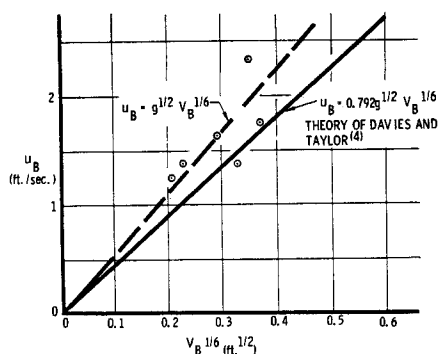


Fig. 9. Void velocity correlation.

trapolating results of one fluidized system to another, it is believed that the results obtained on two-phase flow and on the properties of the dense phase are quite general for other systems with well-established aggregative mode of fluidization. This conclusion is supported by previous experience on fluidized beds. The results obtained here on void sizes and frequencies are limited to this one system pending further work. There is some evidence that these parameters are strongly influenced by the apparatus, for example, the type of distributor used.

It would be very interesting to extend the work to other aggregative systems so as to completely verify these conclusions. It would also be worthwhile to extend the work to other fluidizing modes including the intermediate region between aggregative and particulate fluidization. By studying these systems, for example, it might be possible to determine whether a stable dense phase is associated with a given particle separation. Speculations of this nature and numerous others could be tested experimentally with flash X-ray radiography. As interest grows in the application of fluidized systems to unconventional processes, for example, nuclear rocket reactors, refined measurements of this nature are necessary. Although the commercial use of the flash X-ray machine is relatively new, it has become more and more common and should be more generally available in the future for diversified studies. It is hoped that the study presented here will stimulate interest in its use in the fluidized field as well as other related areas.

CONCLUSIONS

Flash X-ray radiography can be used to obtain photographs of the internal structure of fluidized beds. From this type of photograph, basic fluidized bed data can be obtained; these can be compared for consistency with existing fluidized bed theories. In general, the results obtained here were in good agreement with the two-phase theory, as well as more recent fluid bed theories. The important conclusions obtained are:

1. Two-phase flow was present. Except near the bottom of the bed, quite distinct dense and dilute phases were observed. The former consisted of a uniform emulsion of liquidlike properties, whereas the latter consisted of distinct voids.
2. Near the bottom of the bed less definition existed between phases. This region was quite turbulent; it contained no distinct voids; anomalous densities were sometimes observed.
3. The dense phase maintained, on the average, a constant density with flow rate equal to that measured at minimum fluidization. This result strongly supports the two-phase theory of fluidization.
4. Void size increased with flow rate in qualitative agreement with the two-phase flow theory.

5. In many cases, void shapes were of the spherical cap type; this observation supports theories of flow through a liquidlike emulsion of zero viscosity and surface tension.

6. Void velocities were proportional to the sixth root of the volume and agreed quite well with the theory of bubble flow of Davies and Taylor (4).

The present work considered only one material and one fluidizing medium. Future studies should consider other systems as a basis of providing further support for existing theories. By the use of flash X-ray radiography, which is a powerful tool for motion resolution, the present techniques can be extended without difficulty to a variety of other measurements.

ACKNOWLEDGMENT

The authors wish to thank W. L. Barrett for helpful discussions. The assistance of D. F. Spencer and K. D. Fridell with the operation of the flash X-ray units is gratefully acknowledged. Assistance in design of the equipment and performance of the experiments was rendered at various times by W. A. Freer, F. C. O'Brien, W. H. Taylor, and C. K. Brown.

NOTATION

- f = void frequency, No./sec.
 G = mass flow rate, lb./sq. ft./sec.
 g = acceleration of gravity, ft./sec./sec.
 L = bed height, ft. or in.
 mf = subscript indicating at a minimum fluidization velocity
 t = time, sec.
 u_B = void rise velocity, ft./sec.
 V_B = void volume, cu. ft.
 v = fluid velocity, ft./sec.
 w = flow rate, lb./sec.
 y = void diameter or typical dimension, ft.
 z = distance above distributor, ft.
 ρ = fluid density, lb./cu. ft.

LITERATURE CITED

1. Harrison, D., J. F. Davidson, and J. W. deKock, *Trans. Inst. Chem. Engrs.*, **39**, 202 (1961).
2. Jackson, R., *ibid.*, **41**, 13 (1963).
3. *ibid.*, **22**.
4. Davies, R. M., and Sir Geoffrey Taylor, *Proc. Roy. Soc. (London)*, **A200**, 375 (1950).
5. Rowe, P. N., and B. A. Partridge, Unclassified Report AERE-R 3846, Atomic Energy Research Establishment, Harwell (October, 1961).
6. Toomey, R. D., and H. F. Johnstone, *Chem. Eng. Progr.*, **48**, 220 (1952).
7. Morse, R. D., and C. O. Ballou, *ibid.*, **47**, 199 (1951).
8. Yasui, George, and L. N. Johanson, *A.I.Ch.E. Journal*, **4**, 445 (1958).
9. Baumgarten, P. K., and R. L. Pigford, *ibid.*, **6**, 115 (1960).
10. Wace, P. F., and S. J. Burnett, *Trans. Inst. Chem. Engrs.*, **39**, 168 (1961).
11. Davidson, J. F., R. C. Paul, M. J. S. Smith, and H. A. Duxbury, *ibid.*, **37**, 323 (1959).
12. Harrison, D., and L. S. Leung, *ibid.*, **40**, 146 (1962).
13. Romero, J. B., and D. W. Smith, Document D2-23416, The Boeing Company, Seattle, Washington (1964).
14. Howieson, J. L., R. E. Anderson, W. P. Dyke, and E. J. Grundhauser, *Aerospace Med.*, **34**, 494 (1963).
15. Ergun, Sabri, and A. A. Orning, *Ind. Eng. Chem.*, **41**, 1179 (1949).
16. Romero, J. B., and L. N. Johanson, *Chem. Eng. Progr. Symposium Ser.*, **58**, 28 (1962).
17. Rowe, P. N., *Trans. Inst. Chem. Engrs.*, **39**, 175 (1961).
18. —, and G. A. Henwood, *ibid.*, **43**.

Manuscript received August 18, 1964; revision received December 2, 1964; paper accepted December 23, 1964.